ELSEVIER

Journal of Alloys and Compounds 275–277 (1998) 113–117

Journal of ALLOYS AND COMPOUNDS

Preparation and characterization of alkali- and alkaline earth-based rare earth sulfides

H. Laronze[a,*], A. Demourgues[a], A. Tressaud[a], L. Lozano[a], J. Grannec[a], F. Guillen[a], P. Macaudière[b], P. Maestro[b]

[a] *ICMCB-CNRS, Avenue du Docteur A. Schweitzer, 33608 Pessac, France*
[b] *Rhône–Poulenc CRA, 52 rue de la Haie–Coq, 93308 Aubervilliers, France*

Abstract

Various alkali- and alkaline earth-based cerium and neodymium sulfides (A, Ln)$_3$S$_4$ (A=Li, Na, Ca, Sr) have been prepared by solid state routes. XRD and Ln L$_{III}$-edge EXAFS studies showed that the first and second coordination shells corresponding to the two LnS$_4$ tetrahedra remain quasi-identical whatever the A cations, while the further coordination shells around 4 Å change drastically due to the presence of A cations. Such a cationic distribution may influence the chromatic properties of these compounds. Furthermore, fluorination treatment of Na$_{0.5}$Ce$_{2.5}$S$_4$ sulfide leads to an improvement of the reflectance at λ>640 nm attributed to the presence of CeF$_3$ at the grains surface and to a modification of the microstructure of this material. © 1998 Published by Elsevier Science B.V.

Keywords: Rare earth sulfides; Fluorination treatment; Local environment of rare earths

1. Introduction

The Ce$_2$S$_3$ cerium sesquisulfide and (A, Ce)$_3$S$_4$ related compounds in their high temperature form adopt the γ-Th$_3$P$_4$ type-structure [1] and have potential applications as pigments. The occurrence of A cations occupying cationic sites influences the colour of these compounds. The crystal structure determination of the γ-Ln$_2$S$_3$ phases performed on single crystals as well as the Rietveld refinement of XRD patterns of (A, Ln)$_3$S$_4$ related compounds have been reported by Mauricot et al. [2]. In this structure, the rare earth at 3+ oxidation state as well as the A cations fill statistically the triangulated dodecahedral sites (the 12*a* positions of the *I*$\bar{4}$3*d* space group), whereas the 16*c* positions are fully occupied by sulfur in an octahedral environment of cations. The band structure and especially the energy gap responsible for the observed colour are influenced by the distribution of vacancies in the phases and by cation substitution which lead to an homogenization of the band edges of the valence and conduction bands [3].

The aim of the present work is to determine by powder X-ray diffraction and Ln L$_{III}$-edge EXAFS experiments the structural features of rare earth sulfides. The identification of the Ln–S, Ln–Ln and Ln–A coordination shells will be of great interest to calculate the band structure. Moreover, several studies showed that fluorination treatments where fluorine acts as a strong electron acceptor can be used to induce drastic modifications of the properties of rare earth sulfides [4]. In the present contribution, the effect of fluorination treatments on the chromatic properties of rare earth sulfides has also been investigated by XRD, X-ray photoelectron spectroscopy (XPS) and scanning electron microscopy (SEM).

2. Experimental

2.1. Preparation of materials

Rare earth ternary sulfides with compositions A$_{0.5}$Ln$_{2.5}$S$_4$ (A=Li, Na) and ALn$_2$S$_4$ (A=Ca, Sr) were prepared by reaction of stoichiometric quantities of highest purity rare earth metals, sulfur, alkali or alkaline earth sulfides mixed in an argon glove box. The mixture was put into vitreous carbon crucibles inside a quartz tube sealed under vacuum in order to avoid oxygen traces. The tube was slowly heated at temperature below 400°C during 1

*Corresponding author.

0925-8388/98/$19.00
PII: S0925-8388(98)00286-2

day and raised to 700°C for 1–2 days. The final required reaction temperatures were in the 900–1100°C range.

2.2. Fluorination procedure

The fluorination treatment was performed at room temperature in a conventional experimental set-up previously described [5]. Because of its high reactivity, fluorine gas was mixed with nitrogen (5 to 10% dilution) before reacting with the samples for 5 min to 1 h.

2.3. X-ray diffraction and absorption (EXAFS) experiments

Powder X-ray diffraction (Philips PW 1050/70 diffractometer, Cu Kα radiation) indicated that all samples crystallized with cubic symmetry in the *I*$\bar{4}$3*d* space group. The Rietveld method has been used for refinement of powder XRD data using a pseudo-Voigt profile function. Integrated intensities, positions and structural parameters were refined in the 10–120° (2θ) range using the FULLPROF program. EXAFS spectra at the Ce(Nd) L_{III}-edge were collected on station 7.1 at the Daresbury Synchrotron Radiation Source with beam currents between 150 mA and 250 mA. EXAFS spectra were recorded in transmission mode using a Si (111) monochromator crystal at room temperature and at $T=77$ K. X-ray absorption spectra at the Ce(Nd) L_{III}-edge were reduced to normalized XAFS $\chi(k)$ using Daresbury software and weighted $k^3\chi(k)$ data were analyzed using the EXCURV suite of programs.

2.4. XPS and SEM characterizations

The XPS study was carried out on a 301.SSI spectrometer at LPCM, Pau, France, using a focused monochromatic Al Kα radiation. Microstructure observations were done with a scanning electron microscope (SEM, JEOL 840 SM).

3. Results and discussion

3.1. X-ray diffraction study

The lattice parameter of rare earth sulfides are reported on Table 1. Rare earths, alkali and alkaline earths are distributed over the available cation sites as no superstructure reflections have been identified by XRD and TEM studies. As expected the introduction of large cations such as Sr^{2+} in 12*a* crystallographic sites leads to an increase of the lattice constant, the a parameter raising gradually as a function of the average of cations ionic radii. The XRD pattern of $SrCe_2S_4$ phase has been refined considering the *I*$\bar{4}$3*d* structural hypothesis. The reliability factors used in a standard Rietveld analysis and obtained with fixed isotropic thermal factors ($B_{iso}=0.5$ Å^2) are $R_B=4.7\%$, $R_P=11.5\%$, $R_{WP}=14.2\%$. Experimental and refined X-ray diffraction patterns of this phase are plotted in Fig. 1 and their structural parameters are reported in Table 2. As previously mentioned, the Ce^{3+} and Sr^{2+} cations fill statistically the same crystallographic site which can be described as two overlapping tetrahedra, one larger and the other one smaller. Each Ce(Sr)S_8 dodecahedron shares either one triangular face or one edge with each others.

Table 1
Structural parameters of (A, Ln)$_3S_4$ sulfides (A=Li, Na, Ca, Sr; Ln=Ce, Nd) which adopt the γ-Th_3P_4-type structure (SG: *I*$\bar{4}$3*d*)

Compound	Cell parameter
$Li_{0.5}Nd_{2.5}S_4$	$a=8.498$ (2) Å
$CaNd_2S_4$	$a=8.520$ (3) Å
$Na_{0.5}Nd_{2.5}S_4$	$a=8.526$ (2) Å
$SrNd_2S_4$	$a=8.643$ (4) Å
$Li_{0.5}Ce_{2.5}S_4$	$a=8.601$ (3) Å
$CaCe_2S_4$	$a=8.600$ (2) Å
$Na_{0.5}Ce_{2.5}S_4$	$a=8.638$ (2) Å
$SrCe_2S_4$	$a=8.718$ (1) Å

3.2. EXAFS analysis and discussion

The weighted $k^3\chi(k)$ EXAFS data of $SrCe_2S_4$ compound recorded at $T=77$ K at Ce L_{III}-edge led to the

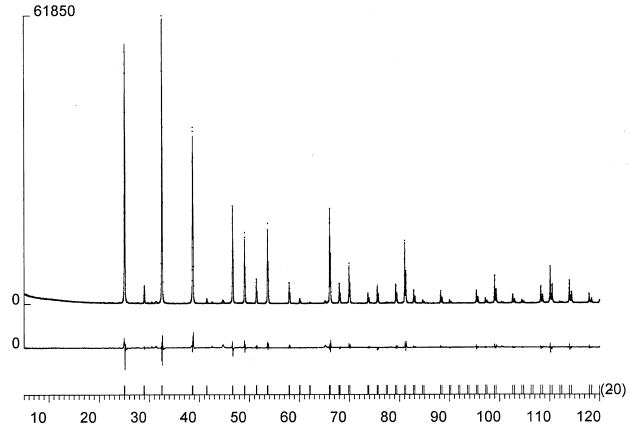

Fig. 1. The observed (...), calculated (–) and difference X-ray profiles of $SrCe_2S_4$ sulfide.

Table 2
Final atomic coordinates and interatomic distances for $SrCe_2S_4$ sulfide (SG: *I*$\bar{4}$3*d*, $a=8.718$ (1) Å)

	x	*y*	*z*
Ce, Sr (12*a*)	3/8	0	1/4
S (I6*c*)	0.0735 (8)	0.0735 (8)	0.0735 (8)
d[Ce(Sr)–S]	4×2.858 (3) Å		
d[Ce(Sr)–S]	4×3.191 (3) Å		
d[Ce(Sr)–Ce(Sr)]	8×4.077 (4) Å		

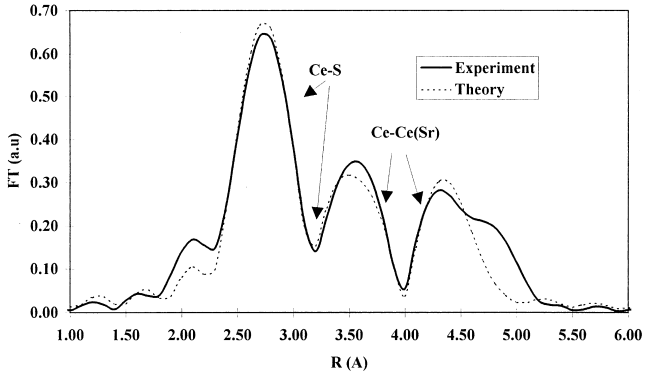

Fig. 2. Fourier transform of the partial radial distribution function for Ce L_{III}-edge EXAFS of $SrCe_2S_4$. The raw experimental data are shown by the solid line and the parameters fit using the environments reported in the text as shown by the dashed line.

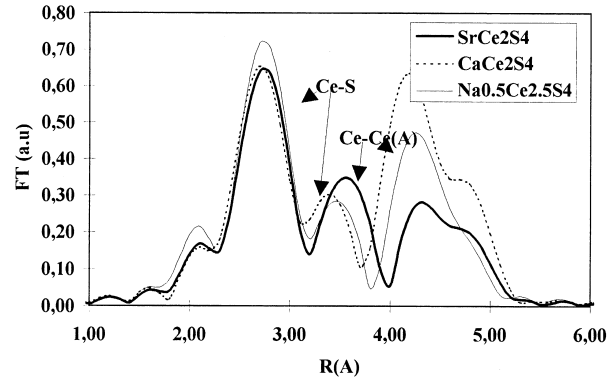

Fig. 3. Experimental Fourier transforms of the partial radial distribution function for Ce L_{III}-edge EXAFS of $Na_{0.5}Ce_{2.5}S_4$, $CaCe_2S_4$ and $SrCe_2S_4$ sulfides.

refinement of four shells up to 4 Å and the determination of nine parameters (radial distance+Debye–Waller factor for each shell+zero energy-shift). The EXAFS data refinement of $SrCe_2S_4$ phase is reported on Fig. 2 and Table 3. The Ce–S bond distances corresponding to the two tetrahedra and the Ce–Ce radial distances obtained by EXAFS are quite comparable to those determined by XRD single crystal study of γ-Ce_2S_3 [2]. The difference which can be noted between Ce–S radial distance corresponding to the larger tetrahedra obtained by EXAFS and XRD studies can be attributed to the presence of larger Sr^{2+} cations in the Ce^{3+} site which leads to averaged structural information in the case of XRD analysis. The cerium coordination spheres of $CaCe_2S_4$ and $Na_{0.5}Ce_{2.5}S_4$ sulfides determined by Ce L_{III}-edge EXAFS data refinement are reported on Table 3 and the Fourier transforms of the EXAFS signals are represented on Fig. 3. The Ce–S coordination shells of Ca- and Na-doped sulfides shift slightly to smaller distances but remain quasi-identical to those of $SrCe_2S_4$. However the Fourier transform magnitude of the coordination shells at 4 and 4.8 Å which can be assigned to Ce–Ce(A) radial distances increase drastically with Ca^{2+} doping and the position of the radial distribution function shift to smaller distances. Such differences are mainly dependent on the nature of the backscatterers (Na, Ca, Sr) which induce various calculated phase-shifts and amplitudes. On the basis of XRD data analysis, the number of Ce or A (Na, Ca, Sr) atoms surrounding Ce at around 4 Å is equal to 8. A distribution of Ce–Ce and Ce–A distances taking into account the chemical composition has been considered in the case of $SrCe_2S_4$ and $CaCe_2S_4$ sulfides. One should notice that whereas the Ce–Sr and Ce–Ce radial distances in $SrCe_2S_4$ are comparable, the refined Ce–Ca distance is shorter than that corresponding to Ce–Ce bond for $CaCe_2S_4$, in good agreement with the decrease of the lattice parameter.

The local environment of Nd in various sulfides ($A_{0.5}Nd_{2.5}S_4$, A=Na, Li; ANd_2S_4, A=Sr, Ca) is also reported in Table 3. As expected the refined radial distances are shorter than those determined in Ce-doped sulfides and are in good agreement with Nd–S distances obtained by XRD analysis on γ-Nd_2S_3 single crystal [1].

In cerium and neodymium sulfides, the incorporation of A cations leads to a modification of Ln–Ln (A) radial distribution while the two Ln–S coordination spheres attributed to the two overlapping tetrahedra remain quasi-identical whatever the A cations. The chromatic properties

Table 3
Ln L_{III}-edge EXAFS data analysis for ternary sulfides

Compound	Ln–S(1) shell		Ln–S(2) shell		Ln–Ln(A) shell	
	Ln–S (Å)	$2\sigma^2$ (Å^2)	Ln–S (Å)	$2\sigma^2$ (Å^2)	Ln–Ln(A) (Å)	$2\sigma^2$ (Å^2)
$CaCeS_4$	2.87	0.007	3.05	0.011	4.03	0.010(Ce)
					3.93	0.014(Ca)
$Na_{0.5}Ce_{2.5}S_4$	2.88	0.006	3.06	0.012	4.05	0.017(Ce)
$SrCe_2S_4$	2.89	0.005	3.08	0.010	4.08	0.011(Ce)
					4.05	0.013(Sr)
$CaNd_2S_4$	2.82	0.007	3.01	0.010	3.99	0.010(Nd)
					3.89	0.019(Ca)
$Li_{0.5}Nd_{2.5}S_4$	2.82	0.010	3.00	0.017	3.97	0.021 (Nd)
$Na_{0.5}Nd_{2.5}S_4$	2.83	0.010	3.00	0.016	3.99	0.017 (Nd)
$SrNd_2S_4$	2.83	0.010	3.02	0.021	4.02	0.013(Nd)
					3.98	0.015(Sr)

of these compounds should be influenced by the structural changes occurring at the rare earth environment, in particular by the various distribution of A cations around 4 Å into the γ-Ln_2S_3 lattice as identified by EXAFS.

3.3. Effect of fluorination treatment on chromatic properties

According to Perrin and Wimmer [3], the observed red color of Ce-based sulfide is related to localized Ce 4f→5d excitations. In order to modify the observed color, a fluorination treatment has been performed on $Na_{0.5}Ce_{2.5}S_4$ phase. Diffuse reflectance spectra recorded on a Cary 17 spectrophotometer in the visible region and obtained for this compound before and after such treatment are shown in Fig. 4. The position of the reflection edge and the reflectance at $\lambda<550$ nm are not modified after fluorination treatment but a steeper slope of the reflectance is observed and the values at $\lambda>640$ nm increase drastically. Thus the fluorination treatment leads to an improvement of the transparency of the sample at $\lambda>640$ nm giving rise to a brighten red color. XRD analysis of the fluorinated sample does not reveal any noticeable change of the pattern associated to the sulfide but the occurrence of weak and broad diffraction lines attributed to cerium fluoride. Moreover a Ce L_{III}-edge EXAFS analysis shows, in addition to the radial distribution of the sulfide, the appearance of a first shell around 2.40 Å associated to Ce–F in CeF_3. In CeF_3, Ce atoms are surrounded by 7 F at distances ranging from 2.395(2) Å to 2.455(2) Å. One should notice that in these conditions the amount of fluoride deduced from the analysis of the number of neighbours corresponding to the first and second shells is high and around 20%. Furthermore the XPS spectra of fluorinated $Na_{0.5}Ce_{2.5}S_4$ phase are drastically different from those of the sulfide before treatment. In the Ce $3d_{5/2}$ XPS region, these spectra are characterized by a satellite on the high binding energy side of the parent lines arising from charge transfer from the ligand valence band into the empty 4f states [6,7]. The intensity of the satellite and the observed binding energies corresponding to fluorinated sample are in very good agreement with those of CeF_3. In addition, a drastic modification of the grain size is observed after treatment, as shown by a SEM study (Fig. 5). The fluorination acts also as a chemical grinding leading to the formation of aggregates with smaller size. However it has not been possible so far to estimate separately the contribution of each effect.

The improvement of chromatic properties of Ce-based sulfides by fluorination treatment can be therefore attributed to both the formation of cerium fluoride at the grain surface which may induce a modification of the refractive

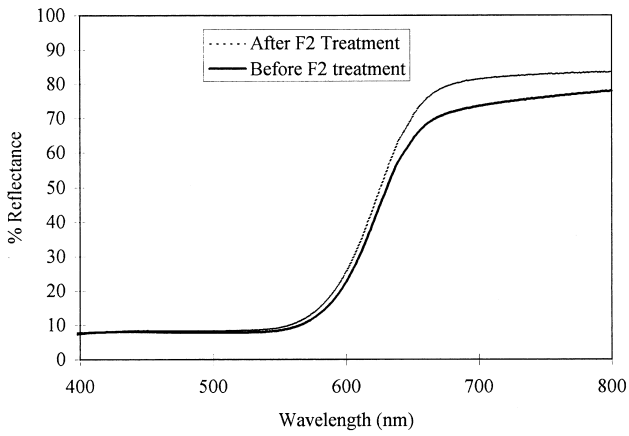

Fig. 4. Diffuse reflectance spectra obtained for $Na_{0.5}Ce_{2.5}S_4$ sulfide before (–) and after (...) fluorination treatment.

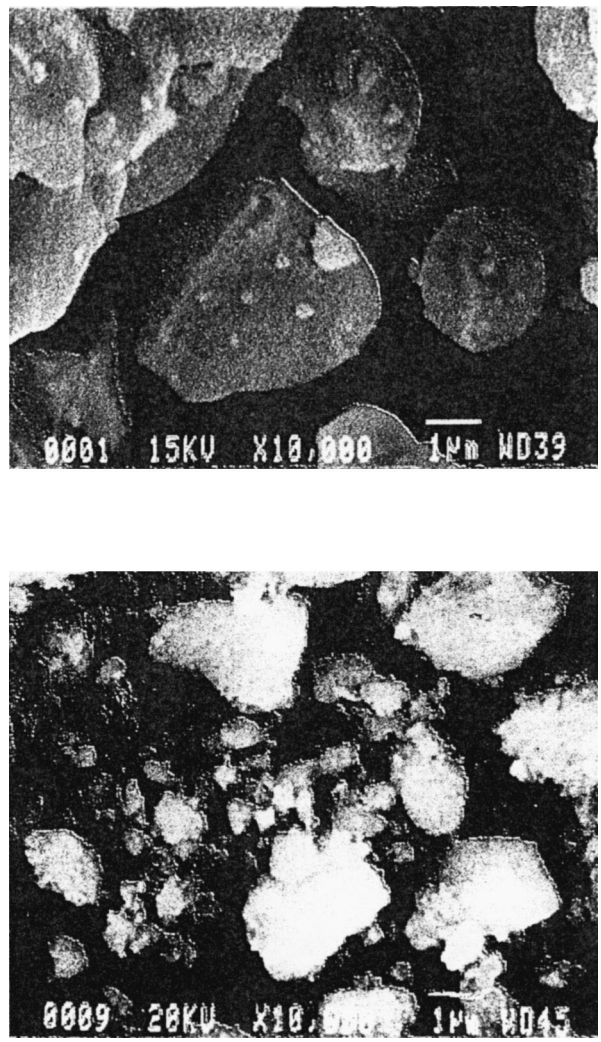

Fig. 5. Microstructure of $Na_{0.5}Ce_{2.5}S_4$ before (above) and after (below) fluorination treatment.

index and the drastic change of the microstructure of materials.

Acknowledgements

C. Guimon (LPCM, France) is acknowledged for performing the XPS experiments.

References

[1] J. Flahaut, L. Domange, M. Patrie,. Bull. Soc. Chim., 1962, p. 2048.
[2] R. Mauricot, P. Gressier, M. Evain, R. Brec, J. Alloys Comp. 223 (1995) 130–138.
[3] M.A. Perrin, E. Wimmer, Phys. Rev. B 54 (1996) 2428–2435.
[4] A. Tressaud, B. Chevalier, L. Piraux, M. Cassart, J. Fluorine Chem. 72 (1995) 165–170.
[5] J. Grannec, L. Lozano, in: P. Hagenmuller (Ed.), Inorganic Solid Fluorides, Academic Press, 1985, p. 17.
[6] S. Kaciulis, A. Latisenka, A. Plesanovas, Surf. Sci. 251-252 (1991) 330–335.
[7] G.K. Wertheim, M. Campagna, Solid State Commun. 26 (1978) 553–556.